

^{17}O NMR study of the local charge state in the hole-doped Cu_2O_3 two-leg spin-ladder $A_{14}\text{Cu}_{24}\text{O}_{41}$ ($A_{14}=\text{La}_6\text{Ca}_8, \text{Sr}_{14}, \text{Sr}_{11}\text{Ca}_3, \text{Sr}_6\text{Ca}_8$)

K. R. Thurber,* K. M. Shen,† and A. W. Hunt

*Department of Physics, Massachusetts Institute of Technology, Cambridge, Massachusetts 02139
and Center for Materials Science and Engineering, Massachusetts Institute of Technology, Cambridge, Massachusetts 02139*

T. Imai‡

*1280 Main Street West, Department of Physics and Astronomy, McMaster University, Hamilton, Ontario, Canada L8S 4M1;
Department of Physics, Massachusetts Institute of Technology, Cambridge, Massachusetts 02139;
and Center for Materials Science and Engineering, Massachusetts Institute of Technology, Cambridge, Massachusetts 02139*

F. C. Chou

*Center for Materials Science and Engineering, Massachusetts Institute of Technology, Cambridge, Massachusetts 02139
(Received 4 November 2002; published 27 March 2003)*

NMR measurements of the ^{17}O nuclear quadrupole interactions $^{17}\nu_Q$ show that the charge environment of the $S=1/2$ Cu_2O_3 two-leg spin-ladder layer of hole-doped $A_{14}\text{Cu}_{24}\text{O}_{41}$ changes dramatically above a certain temperature T^* . This temperature T^* decreases with additional doping and is correlated with the magnetic crossover from the spin gap regime to the paramagnetic regime. We demonstrate that these changes in $^{17}\nu_Q$ are consistent with an increase in the effective hole concentration in the Cu_2O_3 two-leg ladder above T^* . The effective hole concentration increases primarily in the oxygen $2p\sigma$ orbitals.

DOI: 10.1103/PhysRevB.67.094512

PACS number(s): 74.25.Nf, 74.72.-h, 76.60.-k

I. INTRODUCTION

The interplay between quantum spin fluctuations and doped holes in the $S=1/2$ CuO_2 square lattice has been a major controversy in high- T_c superconductivity. The discoveries of the spin-liquid ground state with spin gap Δ in the $S=1/2$ Cu_2O_3 two-leg spin ladder,¹ and superconductivity under high pressure in hole-doped ladders,² raise the same question in a reduced dimension. In this paper, we report a detailed study of the ^{17}O and ^{63}Cu nuclear quadrupole interaction tensor $^{17,63}\nu_Q$ in the Cu_2O_3 two-leg ladder layer of the hole-doped ladder-chain compound $A_{14}\text{Cu}_{24}\text{O}_{41}$ ($A = \text{La}_6\text{Ca}_8, \text{Sr}_{14}, \text{Sr}_{11}\text{Ca}_3, \text{Sr}_6\text{Ca}_8$).

The nuclear quadrupole interaction tensor $^{17,63}\nu_Q$ measures the electric-field gradient at the position of the nucleus, and thus probes the local charge environment. We define ν_Q based on the nuclear quadrupole Hamiltonian as³

$$\mathcal{H}_Q = \frac{1}{6} h \nu_Q^z \left[3I_z^2 - I(I+1) + \frac{1}{2} \eta (I_+^2 + I_-^2) \right], \quad (1a)$$

$$\nu_Q^z = \frac{3e^2qQ}{h2I(2I-1)} \quad (1b)$$

$$\nu_Q^x + \nu_Q^y + \nu_Q^z = 0, \quad \eta = \left| \frac{\nu_Q^x - \nu_Q^y}{\nu_Q^z} \right|, \quad (1c)$$

where Q is the quadrupole moment of the nucleus and I is the spin of the nucleus ($I=3/2$ for $^{63,65}\text{Cu}$, $I=5/2$ for ^{17}O). eq is the electric-field gradient at the site of the nucleus along the principal axis z of the tensor,

$$eq = \sum_i \frac{\delta^2}{\delta z^2} \frac{q_i}{r_i} \quad (2)$$

where the summation is taken over all charges including ions, electrons, etc. The asymmetry parameter η is the deviation of the electric-field gradient tensor from axial symmetry.

The electric-field gradient eq is sensitive to changes in the amount and symmetry of the charge distribution. We demonstrate that the charge environment of the hole-doped ladder changes dramatically above a certain temperature T^* somewhat below the spin gap ($T^* \lesssim \Delta$). Our calculations indicate that extra holes moving primarily into oxygen $2p\sigma$ orbitals are necessary to reproduce the temperature dependence of $^{17,63}\nu_Q$ above T^* .

II. EXPERIMENT AND RESULTS

We grew single-crystal samples of undoped $\text{La}_6\text{Ca}_8\text{Cu}_{24}\text{O}_{41}$ (valence of Cu is +2, $S=1/2$) and $\text{Sr}_{14}\text{Cu}_{24}\text{O}_{41}$ (amount of holes $P_L \sim 0.06$ per ladder Cu at room temperature⁴) using the floating zone technique. For $\text{Sr}_{11}\text{Ca}_3\text{Cu}_{24}\text{O}_{41}$ ($P_L \sim 0.12$) and $\text{Sr}_6\text{Ca}_8\text{Cu}_{24}\text{O}_{41}$ ($P_L \sim 0.17$), we uniaxially aligned ceramic powder in epoxy along the b axis. All of the samples were enriched with ^{17}O isotope by annealing in $^{17}\text{O}_2$ gas at 900°C . We conducted most of the NMR measurements at 7 or 9 T. We assigned the three sets of ^{17}O NMR signals to the O(1) leg and O(2) rung sites (see Fig. 1) and the additional oxygen site in the CuO_2 chain layer based on the symmetry and temperature dependence of the $^{17}\nu_Q$ and NMR Knight shift tensors.⁵ The quadrupole tensors, $^{17,63}\nu_Q$, are discussed below.

In Fig. 2(a), we present the b -axis component of the oxy-

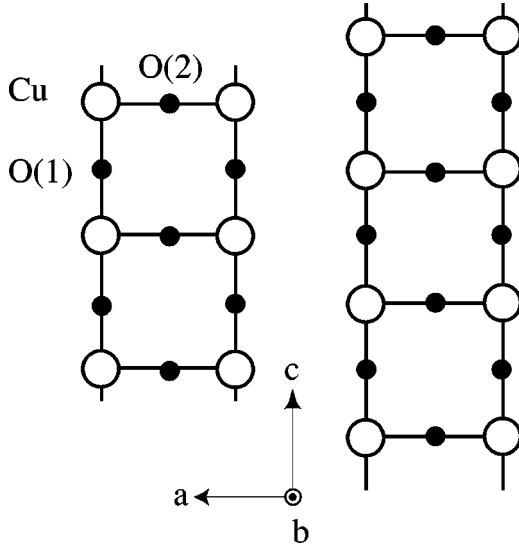


FIG. 1. Structure of two-leg ladder layer of $A_{14}Cu_{24}O_{41}$. Open and closed circles represent Cu and O atoms, respectively.

gen nuclear quadrupole interaction $^{17}\nu_Q[b]$ for the O(1) ladder leg site. Figure 2(b) shows the asymmetry parameter η of $Sr_{14}Cu_{24}O_{41}$ as a function of temperature. A dramatic change in $^{17}\nu_Q$ occurs only for the doped samples, while the undoped $La_6Ca_8Cu_{24}O_{41}$ exhibits a minor decrease of $^{17}\nu_Q$ due to thermal expansion. We define the temperature where this dramatic change begins as T^* and estimate $T^* = 210$ K for $Sr_{14}Cu_{24}O_{41}$ and 140 K for $Sr_{11}Ca_3Cu_{24}O_{41}$. For $Sr_6Ca_8Cu_{24}O_{41}$, $^{17}\nu_Q$ is changing even down to the lowest temperature ($T^* < 10$ K). We also observed a similar dramatic change in temperature dependence at T^* for $^{17}\nu_Q$ at the O(2) ladder rung site for these samples (Fig. 3) and for

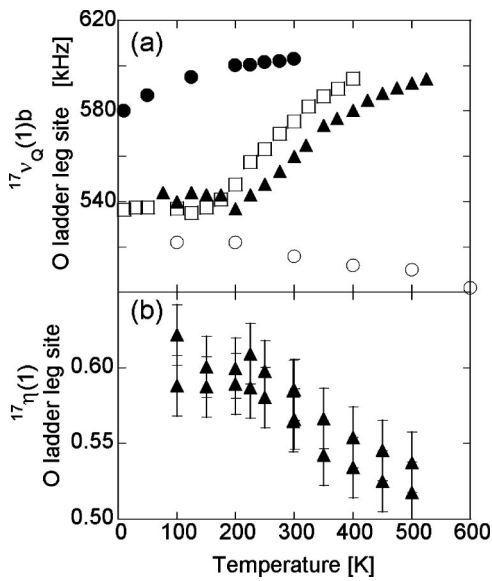


FIG. 2. (a) Temperature dependence of $^{17}\nu_Q(1)[b]$ at O(1) ladder leg site in $La_6Ca_8Cu_{24}O_{41}$ (\circ), $Sr_{14}Cu_{24}O_{41}$ (\blacktriangle), $Sr_{11}Ca_3Cu_{24}O_{41}$ (\square), and $Sr_6Ca_8Cu_{24}O_{41}$ (\bullet). (b) $^{17}\eta(1)$ in $Sr_{14}Cu_{24}O_{41}$. (Double η values caused by slight splitting in ^{17}O lines.)

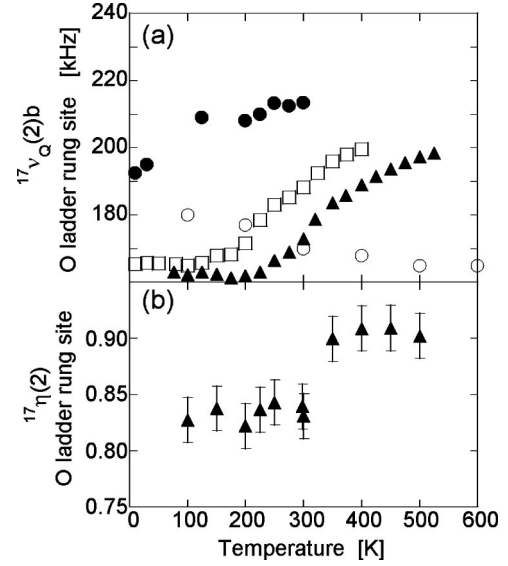


FIG. 3. (a) Temperature dependence of $^{17}\nu_Q(2)[b]$ at O(2) ladder rung site in $La_6Ca_8Cu_{24}O_{41}$ (\circ), $Sr_{14}Cu_{24}O_{41}$ (\blacktriangle), $Sr_{11}Ca_3Cu_{24}O_{41}$ (\square), and $Sr_6Ca_8Cu_{24}O_{41}$ (\bullet). (b) $^{17}\eta(2)$ in $Sr_{14}Cu_{24}O_{41}$.

$^{63}\nu_Q$ at the copper site in $Sr_{14}Cu_{24}O_{41}$.^{6,7} Extremely broad ^{63}Cu NMR line shapes in $La_6Ca_8Cu_{24}O_{41}$ and $Sr_{14-x}Ca_xCu_{24}O_{41}$ have prevented us from measuring $^{63}\nu_Q$ accurately.

In order to understand the dramatic temperature dependence of $^{17}\nu_Q$, we divide the electric-field gradient eq based on a standard ionic picture into two contributions,⁸

$$eq = eq_{\text{hole}} + (1 - \gamma)eq_{\text{lattice}}. \quad (3)$$

The first contribution, eq_{hole} , arises from holes in orbitals of the ion itself. An isotropic distribution of charge, such as from a filled electron shell, will not produce an electric-field gradient, but unfilled shells can. If there is one hole in an oxygen $2p$ orbital, the electric-field gradient at the nucleus is axial with the largest component along the lobe of the p orbital, $\nu_Q = (\frac{3}{20})(\frac{4}{3})e^2Q\langle r^{-3} \rangle$. For our calculations, we take $\langle r^{-3} \rangle = 3.63$ atomic units, which is 70% of the value for a free atom.^{9,10} This results in a nuclear quadrupole interaction of (2.66, -1.33, -1.33) MHz for $^{17}O 2p_x$, for example. Similarly, one hole in the $^{63}Cu 3d_{x^2-y^2}$ orbital produces the nuclear quadrupole interaction $\approx (-38.5, -38.5, 77)$ MHz.^{11,12} The second contribution to the electric-field gradient in Eq. (2), eq_{lattice} , arises from the charges of the other ions of the crystal. This electric field is then modified by the distortion which it creates in the electronic orbitals of the observed ion itself. This effect is accounted for by the Sternheimer antishielding factor γ . For CuO_2 planes in high- T_c superconductors, the value of γ is known to be $^{63}\gamma \approx -20$ and $^{17}\gamma \approx -9$ for ^{63}Cu and ^{17}O , respectively.^{10,12} To calculate the lattice contribution to the electric-field gradient eq_{lattice} , we treat the ionic charges as point charges at their lattice locations.¹³ The electric-field gradient resulting from these point charges is then summed over the lattice out to a radius sufficient to achieve a stable value (typically 50 to 100

lattice spacings). For example, lattice point charge calculations of the electric-field gradient for the undoped material, La₆Ca₈Cu₂₄O₄₁, were done with ionic charges for the (La,Ca) site +2.429, Cu +2, and O -2. Oxygen results for $\gamma = -8$ are (-193, +564, -371) kHz for the O(1) site and (-713, +331, +381) kHz for the O(2) site, in rough agreement with the experimental values (± 60 , ± 516 , $\mp 540 \pm 40$) and (∓ 690 , ± 170 , $\pm 540 \pm 40$) kHz at 291 K. For the copper ladder site, using $\gamma = -20$ and an axial quadrupole interaction from the one hole in the $3d_{a^2-c^2}$ orbital of 77 MHz,¹² point charge calculations give (+1.1, +16.9, -17.9) MHz in reasonable agreement with (∓ 3.3 , ± 16.8 , ∓ 13.5) MHz from measurements at room temperature. The oxygen quadrupole interaction $^{17}\nu_Q$ of the undoped material La₆Ca₈Cu₂₄O₄₁, shows a steady decrease with increasing temperature.

In contrast, for the doped materials, $^{17}\nu_Q$ has a dramatically different temperature dependence. In the following paragraphs, we examine the possible causes for the temperature dependence and conclude that redistribution of the doped holes is responsible. In principle, the observed change in electric-field gradient could arise from changes in one or more of the three parts of Eq. (2), eq_{lattice} , γ , and eq_{hole} . A change in the lattice contribution, eq_{lattice} , would be caused by a change in the crystal structure or lattice parameters as a function of temperature. As discussed by Carretta *et al.*,⁶ the change in lattice parameters as a function of temperature from 293 K to 520 K can account for less than 1% change in $^{63}\nu_Q$, while the experimental change is about 15%. Similarly, we found that the change of lattice parameters would indicate a change of any component of $^{17}\nu_Q$ of 1.5% or less, while the experimentally observed change is as much as 20%. In addition, the sign of the temperature dependence of $^{17}\nu_Q$ is opposite to what would be expected from lattice expansion. As the lattice expands at higher temperatures, the electric-field gradient from the lattice will generally decrease as we see in undoped La₆Ca₈Cu₂₄O₄₁. Clearly, the change in lattice parameters cannot account for the change in quadrupole interaction. Another possibility is that there is a local distortion in the crystal structure. Our analysis using point charge calculations indicates that a local lattice distortion will not produce the experimentally measured sign of the temperature dependence at both the copper and two oxygen sites. The observed Cu $^{63}\nu_Q$ temperature dependence would require an increase in Cu-O bond length, while the O $^{17}\nu_Q$ would require a decrease. More complicated lattice distortions involving further neighboring atoms do not overcome this. Thus, lattice changes are not responsible for the large change in electric-field gradient.

A second possible source for a change in electric-field gradient is a change in the Sternheimer antishielding factor γ . However, Shimizu¹² showed that $^{63}\gamma = -20$ for copper does not vary significantly between copper oxide materials with doping and temperature. Furthermore, our point charge calculations reproduced both $^{63}\nu_Q$ and $^{17}\nu_Q$ tensors of undoped La₆Ca₈Cu₂₄O₄₁ with $^{63}\gamma = -20$ and $^{17}\gamma = -8$, very close to values known for high-T_c cuprates, $^{63}\gamma = -20$,

$^{17}\gamma = -9$. Therefore, we conclude that temperature dependent $^{63,17}\gamma$ in hole-doped ladders is very unlikely.

The third and only remaining possibility is that a change in the hole concentration in the ladder Cu₂O₃ layer changes eq_{hole} of the doped samples. Unlike lattice changes, additional holes can account for the signs and symmetry of the $^{17,63}\nu_Q$ temperature dependence. In the following, we will estimate the change in local hole concentration in the Cu₂O₃ ladder required to account for the changes in the electric-field gradient.

Additional holes affect the electric-field gradient in two ways. First, a hole produces an electric-field gradient at the nuclear site of its own atom through eq_{hole} of Eq. (2). Second, a hole changes the charge of the ion, altering the charge environment of neighboring atoms. This changes the lattice electric-field gradient eq_{lattice} for neighboring atoms. We calculate the effect of the holes on the neighboring atoms by point-charge lattice summations using the values of γ estimated for La₆Ca₈Cu₂₄O₄₁. For our calculations, we consider the possibility of holes in the oxygen 2*p* orbitals of both oxygen sites and in the copper 3*d*_{*a*²-*c*²} or 3*d*_{*b*²-*r*²} orbitals. The subscripts *a*, *b*, and *c* refer to the crystal axes where *b* is perpendicular to the ladder layer, *a* is along the rungs of the ladder, and *c* is along the ladder direction. We determine the amount of doped holes in each oxygen and copper orbital from $^{63}\nu_Q$ and the tensor components of $^{17}\nu_Q(1,2)$ considering consistently both the on-site effect of a hole on its own nucleus and the indirect effect of a hole on nearby atoms. The resulting equations relating the change in $^{17,63}\nu_Q$ to the change in hole concentration Δh in each orbital are (in units of MHz)

$$\begin{aligned} \Delta^{17}\nu_Q(1)[b] = & -1.33\Delta h_{2p_a(1)} - 1.33\Delta h_{2p_c(1)} - 0.55\Delta h_{\text{Cu}} \\ & - 0.19\Delta h_{\text{O}(1)} - 0.14\Delta h_{\text{O}(2)} - 0.20\Delta h_{\text{total}}, \end{aligned} \quad (4a)$$

$$\begin{aligned} \Delta^{17}\nu_Q(1)[c] = & -1.33\Delta h_{2p_a(1)} + 2.66\Delta h_{2p_c(1)} + 0.49\Delta h_{\text{Cu}} \\ & + 0.12\Delta h_{\text{O}(1)} + 0.05\Delta h_{\text{O}(2)} + 0.10\Delta h_{\text{total}}, \end{aligned} \quad (4b)$$

$$\begin{aligned} \Delta^{17}\nu_Q(2)[b] = & -1.33\Delta h_{2p_a(2)} - 1.33\Delta h_{2p_c(2)} - 0.45\Delta h_{\text{Cu}} \\ & - 0.29\Delta h_{\text{O}(1)} - 0.04\Delta h_{\text{O}(2)} - 0.17\Delta h_{\text{total}}, \end{aligned} \quad (4c)$$

$$\begin{aligned} \Delta^{17}\nu_Q(2)[c] = & -1.33\Delta h_{2p_a(2)} + 2.66\Delta h_{2p_c(2)} - 0.30\Delta h_{\text{Cu}} \\ & + 0.10\Delta h_{\text{O}(1)} + 0.06\Delta h_{\text{O}(2)} + 0.10\Delta h_{\text{total}}, \end{aligned} \quad (4d)$$

$$\begin{aligned} \Delta^{63}\nu_Q[b] = & 77\Delta h_{3d_{a^2-c^2}} + 12\Delta h_{\text{Cu}} + 35\Delta h_{\text{O}(1)} + 14\Delta h_{\text{O}(2)} \\ & + 13\Delta h_{\text{total}}; \end{aligned} \quad (4e)$$

$$\Delta h_{\text{O}(1,2)} = \Delta h_{2p_a(1,2)} + \Delta h_{2p_c(1,2)}, \quad (4f)$$

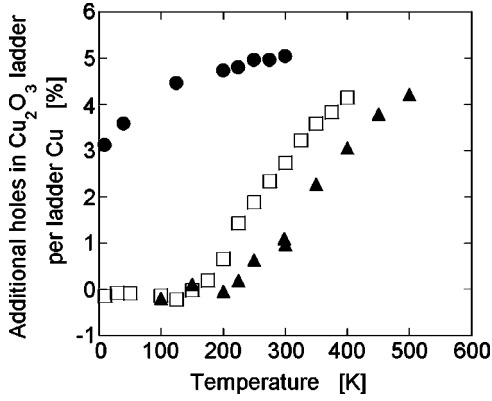


FIG. 4. Additional observed holes in the Cu_2O_3 ladder layer per ladder Cu as deduced from ^{17}O and ^{63}Cu ν_Q for $\text{Sr}_{14}\text{Cu}_{24}\text{O}_{41}$ (\blacktriangle), $\text{Sr}_{11}\text{Ca}_3\text{Cu}_{24}\text{O}_{41}$ (\square), and $\text{Sr}_6\text{Ca}_8\text{Cu}_{24}\text{O}_{41}$ (\bullet).

$$\Delta h_{\text{Cu}} = \Delta h_{3d_{a^2-c^2}}, \quad (4g)$$

$$\Delta h_{\text{total}} = (14/20)\Delta h_{\text{Cu}} + (14/20)\Delta h_{\text{O}(1)} + (7/20)\Delta h_{\text{O}(2)}. \quad (4h)$$

These equations have three types of terms. First, the terms that refer to specific atomic orbitals result from the on-site effect of a hole on its own nucleus. Second, the terms that refer to the holes on specific atomic sites result from the change in the lattice electric-field gradient caused by holes on neighboring atoms in the ladder layer. Third, the final Δh_{total} term in these equations results from the effect on the lattice electric-field gradient of removing these holes from the chain layer. This third contribution is calculated based on the assumption that there are no holes in the ladder layer of $\text{Sr}_{14}\text{Cu}_{24}\text{O}_{41}$ in the low-temperature region below 210 K and that additional holes in the ladder layer are removed evenly from all of the chain layer atoms. For the uniaxially aligned powder samples, we have only measured b axis quadrupole frequency and we assumed that the distribution of holes between the oxygen and copper orbitals was the same as in $\text{Sr}_{14}\text{Cu}_{24}\text{O}_{41}$.

We summarize the total number of additional holes required in the ladder Cu_2O_3 layer to produce the experimentally observed changes of $^{17,63}\nu_Q$ in Fig. 4, and the distribution of the holes between the oxygen $2p$ orbitals and copper $3d$ orbitals in Table I for $\text{Sr}_{14}\text{Cu}_{24}\text{O}_{41}$ at 500 K. The change in hole concentration for $\text{Sr}_{14}\text{Cu}_{24}\text{O}_{41}$ from low temperature to 500 K represents an observed increase of less than one hole in the ladder layer out of the six holes implicit in the $\text{Sr}_{14}\text{Cu}_{24}\text{O}_{41}$ formula unit. Primarily, the holes go into the oxygen $2p\sigma$ orbitals, the O(1) leg site $2p_a(1)$ and $2p_c(1)$ and the O(2) rung site $2p_a(2)$. There is possibly also some hole transfer to the ladder copper site, but there is much

TABLE I. Additional observed holes in ladder layer orbitals of $\text{Sr}_{14}\text{Cu}_{24}\text{O}_{41}$ at 500 K deduced from $^{17,63}\nu_Q$

$\text{O } 2p_a(1)$	$\text{O } 2p_c(1)$	$\text{O } 2p_a(2)$	$\text{O } 2p_c(2)$	$\text{Cu } 3d_{a^2-c^2}$
$1.3 \pm 0.3\%$	$1.3 \pm 0.3\%$	$1.0 \pm 0.3\%$	$0.3 \pm 0.3\%$	$0.9 \pm 0.6\%$

larger uncertainty in the calculation of the holes on the copper site because of the importance of the lattice contribution of the oxygen holes to the calculated $^{63}\nu_Q$.

We emphasize that Fig. 4 just shows the additional holes necessary to account for the temperature dependence of the electric-field gradient. The low-temperature region of ν_Q for $\text{Sr}_{14}\text{Cu}_{24}\text{O}_{41}$ was taken as a starting point from which the additional holes necessary to account for the temperature dependence of $^{17,63}\nu_Q$ are calculated. This is done to avoid uncertainties in the lattice contribution to the electric-field gradient. Lattice point charge calculations are clearly a simplified approximation which prevents an absolute determination of the hole concentration in the ladder Cu_2O_3 layer. However, for $\text{Sr}_6\text{Ca}_8\text{Cu}_{24}\text{O}_{41}$, $^{17}\nu_Q$ is still changing down to the lowest temperature (10 K) and our calculations do suggest that holes are still present in the ladder layer at 10 K as shown in Fig. 4. We emphasize that the physical picture given by this analysis is independent of the lattice point charge calculation and the value of γ . For example, calculating ν_Q without including any lattice contributions does increase the number of holes required in each orbital to account for our measured ν_Q , but does not change the symmetry of the orbitals where the holes reside. From Table I, we see that the majority of the holes reside on the O(1) site [2.6% on O(1), 0.65% on O(2), and 0.9% on Cu site per ladder Cu]. For the O(1) site, the on-site hole contribution is the dominant effect in the calculation and the contribution from the lattice effect of holes on nearby ions is $\leq 25\%$. That the holes primarily reside in oxygen $2p\sigma$ orbitals is consistent with x-ray absorption spectroscopy¹⁴ and other copper oxide materials, such as $\text{YBa}_2\text{Cu}_3\text{O}_7$ and $(\text{La,Sr})\text{CuO}_4$.^{10,15}

III. DISCUSSION

Other measurements of these $\text{A}_{14}\text{Cu}_{24}\text{O}_{41}$ materials also point towards changes in hole concentration at T^* . Optical conductivity measurements⁴ of the Drude peak at low frequency are attributed to carriers in the ladder layer. The temperature dependence of the integral of that peak, which represents N/m^* (carrier number over effective mass), is similar to that of the electric-field gradient. Charge transport^{16,17} shows an anomaly at around T^* for several doping levels as summarized in Fig. 5 and also a possible collective excitation in $\text{Sr}_{14}\text{Cu}_{24}\text{O}_{41}$ below T^* .¹⁸ In addition, magnetic susceptibility^{16,17} indicates that the ladder layer contributes to the susceptibility only above T^* . The mean free path of ladder magnetic excitations also shows a sharp decrease around T^* .¹⁹

Also correlated with the changes in electric-field gradient are magnetic changes seen in the nuclear spin-lattice relaxation rate $1/T_1$ for ^{63}Cu .⁵ $1/T_1$ generally measures low-energy spin fluctuations. As shown in Fig. 6(b), ^{63}Cu $1/T_1$ crosses over from a low-temperature gapped regime where $1/T_1$ roughly follows an activation law $\exp(-\Delta_{T_1}/k_B T)$ to a paramagnetic regime. The onset of the change in the electric-field gradient, T^* , is at the beginning of the crossover from the low-temperature gapped regime to the paramagnetic regime. In addition, for $\text{Sr}_{14}\text{Cu}_{24}\text{O}_{41}$, Takigawa *et al.*⁷ and Carretta *et al.*⁶ noted that for $T \leq 225$ K, the fit of the nuclear

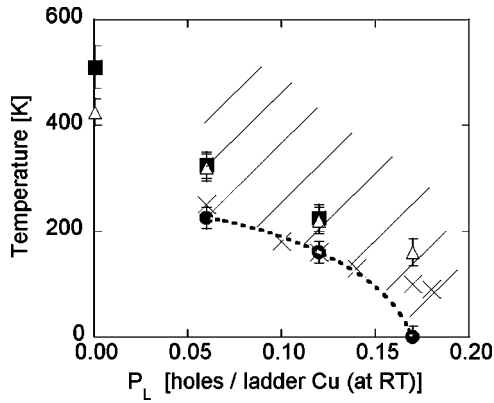


FIG. 5. T^* (●, this work), T_{tran} (×, after Ref. 16), ΔT_1 (△, from Ref. 5), and $\Delta\chi$ (■, from Ref. 5) for various room temperature hole-doping levels P_L [Ref. 4], $\text{La}_6\text{Ca}_8\text{Cu}_{24}\text{O}_{41}$ ($P_L=0$), $\text{Sr}_{14}\text{Cu}_{24}\text{O}_{41}$ ($P_L\sim 0.06$), $\text{Sr}_{11}\text{Ca}_3\text{Cu}_{24}\text{O}_{41}$ ($P_L\sim 0.12$), and $\text{Sr}_6\text{Ca}_8\text{Cu}_{24}\text{O}_{41}$ ($P_L\sim 0.17$). Crosshatched region indicates where hole transfer occurs.

magnetization decay to the standard solution of the rate equations becomes poor, and the ratio $(^{65}1/T_1)/(^{63}1/T_1)$ decreases from $(^{65}\gamma/^{63}\gamma)^2 = 1.15$ indicating that charge fluctuations are contributing to the relaxation. The quadrupolar relaxation is maximum at about 100 K for $\text{Sr}_{14}\text{Cu}_{24}\text{O}_{41}$ indicating that charge fluctuations have slowed down to the NMR frequency.^{6,7} As shown in Fig. 6(a), we found that quadrupolar relaxation is significant below $T \approx \Delta T_1$ for all hole-doped samples. Most likely, these charge fluctuations are associated with very slow hole motion in the ladder plane.

The additional holes that are observed in the Cu_2O_3 lad-

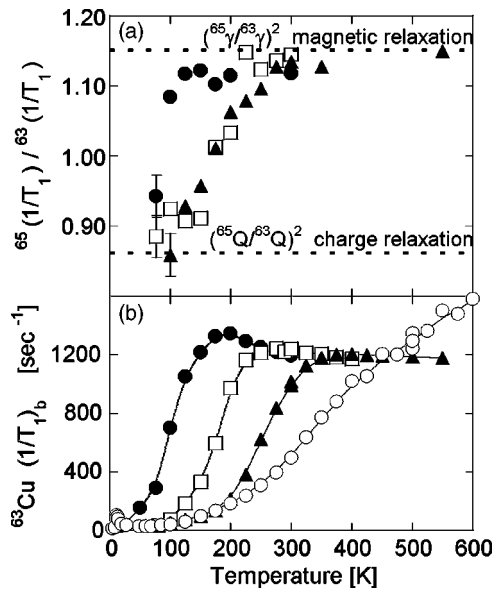


FIG. 6. (a) Temperature dependence of the ratio $^{65}(1/T_1)/^{63}(1/T_1)$ for $\text{Sr}_{14}\text{Cu}_{24}\text{O}_{41}$ (▲), $\text{Sr}_{11}\text{Ca}_3\text{Cu}_{24}\text{O}_{41}$ (□), and $\text{Sr}_6\text{Ca}_8\text{Cu}_{24}\text{O}_{41}$ (●). A few representative error bars shown. (b) $^{63}\text{Cu} (1/T_1)_b$ for $\text{La}_6\text{Ca}_8\text{Cu}_{24}\text{O}_{41}$ (○), $\text{Sr}_{14}\text{Cu}_{24}\text{O}_{41}$ (▲), $\text{Sr}_{11}\text{Ca}_3\text{Cu}_{24}\text{O}_{41}$ (□), and $\text{Sr}_6\text{Ca}_8\text{Cu}_{24}\text{O}_{41}$ (●). Lines are guides for the eye.

der above T^* could arise from two obvious sources: transfer from the chain layer, or delocalization from unobserved regions of the ladder layer. Transfer of holes from the chain layer seems quite plausible because of the coincidence of the temperature of the delocalization of holes on the chain with the appearance of the holes in the ladder layer at T^* . NMR,⁷ ESR,²⁰ and x-ray diffraction experiments²¹ all show that the holes in the chain delocalize at around $T^* = 210$ K for $\text{Sr}_{14}\text{Cu}_{24}\text{O}_{41}$. The ESR experiment also indicates charge ordering of the chain at 170 K for $\text{Sr}_{12}\text{Ca}_2\text{Cu}_{24}\text{O}_{41}$ and at ~ 80 K for $\text{Sr}_9\text{Ca}_5\text{Cu}_{24}\text{O}_{41}$,²⁰ consistent with our observation of hole increase in the ladder layer starting at 140 K for $\text{Sr}_{11}\text{Ca}_3\text{Cu}_{24}\text{O}_{41}$. Transfer of holes from the chain to the ladder layer also explains one apparent discrepancy. Below the chain charge ordering temperature, NMR (Ref. 7) and neutron scattering²² measurements show separated dimers on the chain of $\text{Sr}_{14}\text{Cu}_{24}\text{O}_{41}$. The separated dimer model has six holes per formula unit, which is all of the holes expected in $\text{Sr}_{14}\text{Cu}_{24}\text{O}_{41}$. If no holes move between chain and ladder layers, this does not leave any holes for the ladder layer. This conflicts with the measurement of holes in the ladder plane of $\text{Sr}_{14}\text{Cu}_{24}\text{O}_{41}$ at high temperature by this work and optical conductivity.⁴ Takigawa *et al.*⁷ noted this discrepancy and also pointed out that any nonstoichiometry did not seem large enough to account for this effect. On the other hand, if holes do move from the chain layer to the ladder layer with increasing temperature, there is a consistent picture: the holes are all on the chain below 210 K and gradually transfer to the ladder plane at higher temperatures, as shown in Fig. 4.

The second possible source of holes is delocalization from unobserved regions of the ladder layer. The hole concentration in the Cu_2O_3 ladder below T^* can be smaller for the majority of the Cu and O(1,2) sites, if holes are localized within the NMR time scale ($\sim \mu\text{sec}$) below T^* . One possible piece of evidence in support of this possibility is the existence of a collective excitation in the conductivity of $\text{Sr}_{14}\text{Cu}_{24}\text{O}_{41}$ below ~ 170 K.¹⁸ This might indicate the motion of pinned charges in the ladder layer. However, the origin of the collective excitation is not clear. In addition, the spectral weight of the conductivity peak is at least six orders of magnitude smaller than that expected using $P_L \sim 0.07$ and an effective mass equal to the free electron mass. Thus, this excitation may involve a very small number of holes. The anomalies in charge transport and magnetic susceptibility measurements have been interpreted as charge localization at T^* ,¹⁷ but this does not seem to account for the NMR results. This scenario requires NMR line broadening or splitting around T^* due to the localization of holes, but we did not observe any significant broadening of the NMR line shape around T^* . Some NMR quadrupole satellite lines are slightly split, but the size of the splitting is temperature independent (shown by η in Fig. 2). Additionally, the peak in quadrupole relaxation for $\text{Sr}_{14}\text{Cu}_{24}\text{O}_{41}$ (Ref. 7) implies that the hole motion slows down to the NMR frequency only at around 100 K, so the charge dynamics at higher temperatures such as $T^* = 210$ K should be faster than the NMR time scale, not slower. Therefore, this delocalization scenario does not seem as consistent as the possibility of holes transferring from the

chain to the ladder layer. However, the quadrupolar relaxation does imply that the ladder layer has nearby charge fluctuations, so it is possible that some holes do localize on the ladder layer.

IV. CONCLUSION

We report a detailed study of ^{17}O and ^{63}Cu ν_Q measurements on $A_{14}\text{Cu}_{24}\text{O}_{41}$ two-leg ladder sites. The charge environment of the ladder layer for the doped samples dramatically changes at temperatures above T^* . An increase in the effective hole concentration is observed in the ladder layer above T^* , primarily in oxygen $2p\sigma$ orbitals. We suggest that these holes may be transferred from the chain layer. The change in the charge environment of the ladder layer occurs

at the beginning of the magnetic crossover from the low-temperature gapped region to the high-temperature paramagnetic region. This suggests that spin and charge degrees of freedom are closely connected in the hole-doped two-leg Cu_2O_3 ladder of $A_{14}\text{Cu}_{24}\text{O}_{41}$. Holes are excluded from the majority of the ladder plane below T^* , when the two-leg ladder is in the low-temperature spin-gapped state. Above T^* , the spin-gapped state is disturbed by holes and spin excitations are seen in $1/T_1$ and magnetic susceptibility.

ACKNOWLEDGMENTS

Early parts of this work were supported by NSF DMR 99-71264, NSF DMR 98-08941, and NSF DMR 96-23858.

*Present address: U.S. Army Research Lab, Adelphi, MD.

†Present address: Department of Applied Physics, Stanford University, Stanford, CA.

‡Permanent address: Department of Physics and Astronomy, McMaster University, Hamilton, Ontario, Canada.

¹M. Azuma, Z. Hiroi, M. Takano, K. Ishida, and Y. Kitaoka, Phys. Rev. Lett. **73**, 3463 (1994).

²M. Uehara, T. Nagata, J. Akimitsu, H. Takahashi, N. Môri, and K. Kinoshita, J. Phys. Soc. Jpn. **65**, 2764 (1996).

³A. Abragam, *Principles of Nuclear Magnetism* (Oxford University Press, Oxford, 1961).

⁴T. Osafune, N. Motoyama, H. Eisaki, and S. Uchida, Phys. Rev. Lett. **78**, 1980 (1997); H. Eisaki, N. Motoyama, K.M. Kojima, S. Uchida, N. Takeshita, and N. Mori, Physica C **341–348**, 363 (2000); K.M. Kojima, N. Motoyama, H. Eisaki, and S. Uchida, J. Electron Spectrosc. Relat. Phenom. **117–118**, 237 (2001); (unpublished).

⁵T. Imai, K.R. Thurber, K.M. Shen, A.W. Hunt, and F.C. Chou, Phys. Rev. Lett. **81**, 220 (1998).

⁶P. Carretta, P. Ghigna, and A. Lascialfari, Phys. Rev. B **57**, 11 545 (1998); P. Carretta, S. Aldrovandi, R. Sala, P. Ghigna, and A. Lascialfari, *ibid.* **56**, 14 587 (1997).

⁷M. Takigawa, N. Motoyama, H. Eisaki, and S. Uchida, Phys. Rev. B **57**, 1124 (1998).

⁸M.H. Cohen and F. Reif, Solid State Phys. **5**, 321 (1957).

⁹J.S.M. Harvey, Proc. R. Soc. London, Ser. A **285**, 581 (1965).

¹⁰M. Takigawa, P.C. Hammel, R.H. Heffner, Z. Fisk, K.C. Ott, and J.D. Thompson, Phys. Rev. Lett. **63**, 1865 (1989).

¹¹C.H. Pennington, D.J. Durand, C.P. Slichter, J.P. Rice, E.D. Bukowski, and D.M. Ginsberg, Phys. Rev. B **39**, 2902 (1989).

¹²T. Shimizu, J. Phys. Soc. Jpn. **62**, 772 (1993).

¹³E.M. McCarron, III, M.A. Subramanian, J.C. Calabrese, and R.L. Harlow, Mater. Res. Bull. **23**, 1355 (1988); T. Siegrist, L.F.

Schneemeyer, S.A. Sunshine, and J.V. Waszczak, *ibid.* **23**, 1429 (1988).

¹⁴N. Nücker, M. Merz, C.A. Kuntscher, S. Gerhold, S. Schuppler, R. Neudert, M.S. Golden, J. Fink, D. Schild, S. Stadler, V. Chakarian, J. Freeland, Y.U. Idzerda, K. Conder, M. Uehara, T. Nagata, J. Goto, J. Akimitsu, N. Motoyama, H. Eisaki, S. Uchida, U. Ammerahl, and A. Revcolevschi, Phys. Rev. B **62**, 14 384 (2000).

¹⁵N. Nücker, J. Fink, J.C. Fuggle, P.J. Durham, and W.M. Temmerman, Phys. Rev. B **37**, 5158 (1988); A. Fujimori, E. Takayama-Muromachi, Y. Uchida, and B. Okai, *ibid.* **35**, 8814 (1987); K. Schwarz, C. Ambrosch-Draxl, and P. Blaha, *ibid.* **42**, 2051 (1990); K. Hanzawa, J. Phys. Soc. Jpn. **62**, 3302 (1993); G. Zheng, Y. Kitaoka, K. Ishida, and K. Asayama, *ibid.* **64**, 2524 (1995).

¹⁶S.A. Carter, B. Batlogg, R.J. Cava, J.J. Krajewski, W.F. Peck, Jr., and T.M. Rice, Phys. Rev. Lett. **77**, 1378 (1996).

¹⁷T. Adachi, K. Shiota, M. Kato, T. Noji, and Y. Koike, Solid State Commun. **105**, 639 (1998).

¹⁸H. Kitano, R. Inoue, T. Hanaguri, A. Maeda, N. Motoyama, M. Takaba, K. Kojima, H. Eisaki, and S. Uchida, Europhys. Lett. **56**, 434 (2001).

¹⁹A.V. Sologubenko, K. Giannó, H.R. Ott, U. Ammerahl, and A. Revcolevschi, Phys. Rev. Lett. **84**, 2714 (2000).

²⁰V. Kataev, K.-Y. Choi, M. Grüninger, U. Ammerahl, B. Büchner, A. Freimuth, and A. Revcolevschi, Phys. Rev. B **64**, 104422 (2001).

²¹T. Fukuda, J. Mizuki, and M. Matsuda, Phys. Rev. B **66**, 012104 (2002).

²²M. Matsuda, T. Yoshida, K. Kakurai, and G. Shirane, Phys. Rev. B **59**, 1060 (1999).